Proc. Natl. Acad. Sci. USA
Vol. 95, pp. 8436–8440, July 1998
Chemistry

Hydration for a series of hydrocarbons

RAYMOND D. MOUNTAIN* AND D. THIRUMALAI*†

*Physical and Chemical Properties Division, National Institute of Standards and Technolgy, Gaithersburg, MD 20899; and †Department of Chemistry and Biochemistry, Institute for Physical Science and Technology, University of Maryland, College Park, MD 20742

Communicated by Johanna M. H. Levelt Sengers, National Institute of Standards and Technology, Gaithersburg, MD, May 18, 1998 (received for review February 18, 1998)

ABSTRACT **The hydrophobic hydration in a series of hydrocarbons is probed by using molecular dynamics simulations. The solutes considered range from methane to octane. Examination of the shapes of the hydration shell suggests that there is no single stable structure surrounding these solutes. The structure of the water molecules around the solute is not significantly perturbed, even for octane, and the hydrogen bond network is essentially preserved. The solutes are accommodated in the voids of the tetrahedral network of water in such a way as to leave the local environment almost intact. The hydrophobic hydration arises primarily because of the plasticity of the hydrogen bond network. Even for octane we find very little evidence for water-mediated interactions between nonbonded carbon atoms, leading us to suggest that the transition to globular conformations can only occur for very long, linear hydrocarbon chains.**

INTRODUCTION

It is thought that the hydrophobic interaction between nonpolar species is the major driving force in the self-assembly of proteins (1). The hydrophobic interaction refers to the free energy increase upon transfer of nonpolar species from nonpolar solvents to water (2). Because water is a poor solvent for nonpolar species, the potential of mean force between two nonpolar moieties in water has an attractive minimum. Numerous studies investigating the origin of the hydrophobic interaction exist (3–10). Regardless of the origin of the effective attraction between nonpolar solutes in water, it is clear that to dissolve them, a cavity of appropriate size needs to be created to accommodate the solute (11). A measure of the hydrophobic interaction is the reversible quasi-static work required to open a cavity in the solvent (8, 9). The possible existence of such well defined cavities (usually assumed to be spherical) has formed the basis for describing solubilities of simple nonpolar molecules in terms of theories like the scaled particle theory (12, 13) and other molecular theories (7). Further attempts to quantitatively understand hydrophobicity have been made by Pratt and coworkers (8) by examining the statistics of cavity size distributions. These calculations reveal that, although the most probable cavity size is the same in water and other nonpolar liquids (n-hexane for example), the fluctuations in the size of that volume are considerably larger in hexane than in water. The relatively narrow distribution of cavity sizes in water leads to a decrease in the solubility of all but the very small-sized solute molecules. This point of view should be contrasted with suggestions (14) that the hydrophobic interaction can be understood in terms of the small size of the water molecule alone and that the intrinsic structure of the water molecule is relatively unimportant. The latter approaches basically ignore the hydrogen bonding that dominates the short range order in water. Thus, it is of interest to investigate the intermediate-size case of the solvation of larger hydrocarbons. These studies, which necessarily involve creating a larger cavity in the solvent, can be used to assess the validity of describing hydrophobic interactions purely in terms of cavity statistics.

It is obvious that the probability of creating a large anisotropic cavity to accommodate a solute would decrease with the volume of the solute. Thus, one might expect that large solute molecules would distort the hydration structure at least locally. Such an expectation is borne out in the extreme case of water near a hydrophobic wall simulated under constant volume conditions (15–17). These studies showed that close to the wall there is a loss of one hydrogen bond per molecule. A natural question is how the solvent responds to the presence of large apolar molecules with internal degrees of freedom. There have been relatively few studies describing the nature of solvation of large hydrocarbons (18). Because these hydrocarbon molecules are intrinsically flexible, one may expect that local distortions of water structure are minimized. Our study is intended to investigate the hydrophobic hydration of hydrocarbons and to bridge this gap between hydrophobic walls and small molecules. In particular, we focus on the structural and dynamical shape fluctuations of the hydration shell for a series of hydrocarbons ranging from methane to octane, by using constant volume molecular dynamics simulations. As the alkanes are nearly insoluble in water, the solvent develops a solvation shell that isolates the solute and at the same time provides a minimum disruption of the normal liquid structure. Also, these solutes provide a sequence of systems where "hydrophobic interactions" are significant. An examination of the process that results in the development of this shell is outside the range of the current study.

The Models. Water was represented by the SPC/E model (19). This is a rigid, three-site model. The hydrogen sites are located 0.1 nm from the oxygen site and the HOH angle is 109.47°. The hydrogen sites have charges, $q_H = 0.4238e$, and the oxygen site has a neutralizing charge. There is a Lennard–Jones iteraction between oxygen sites with $\epsilon = 78.24$ K and $\sigma = 0.3166$ nm.

A united atom, site–site interaction model for alkanes has been shown to provide satisfactory estimates for the liquid–vapor coexistence curves for several of the alkanes. A slight variant of this interaction model has been used here to model alkanes from methane, N = 1, to octane, N = 8, in the liquid state (20).

The intramolecular interaction, V_{intra}, consists of four parts:

$$V_{intra} = V_2 + V_3 + V_4 + V_5. \quad \textbf{[1]}$$

The V_2 term contains the harmonic stretch interactions between bonded neighbors,

$$V_2 = \frac{1}{2}\sum_{i=1}^{N-1} \gamma_2 (r_{ij} - d_0)^2, \quad \textbf{[2]}$$

$j = i + 1$, $\gamma_2 = 4.529 \times 10^7$ K/nm^2, and $d_0 = 0.154$ nm. The V_3 term contains the harmonic bend interactions that involve

The publication costs of this article were defrayed in part by page charge payment. This article must therefore be hereby marked "*advertisement*" in accordance with 18 U.S.C. §1734 solely to indicate this fact.

0027-8424/98/958436-5$0.00/0
PNAS is available online at http://www.pnas.org.

adjacent triples of sites,

$$V_3 = \frac{1}{2}\sum_{i=1}^{N-2} \gamma_3(\theta_{ijk} - \theta_0)^2, \quad [3]$$

$j = i+1$, $k = i+2$, and θ_{ijk} is the angle at site j. The parameters are $\theta_0 = 114^\circ$ and $\gamma_3 = 62498$ K/rad^2. The V_4 term contains the torsion interactions that involves adjacent quadruples of sites (21),

$$V_4 = \sum_{i=1}^{N-3}\sum_{l=0,5} C_l \cos^l(\phi), \quad [4]$$

where ϕ is the dihedral angle between the planes defined by the four sites. The values of the coefficients, C_l appearing in V_4 are (in units of Kelvins) 1116, 1462, −1578, −368, 3156, and −3788 for $l = 0$ to $l = 5$. The V_5 term is a Lennard–Jones interaction between sites separated by more than three or more sites,

$$V_5 = \sum_{j=1}^{N-4}\sum_{k=j+4}^{N} V_{LJ}(r_{jk}), \quad [5]$$

with $\epsilon = 114$ K and $\sigma = 0.393$ nm.

The solvent–solute interactions are Lennard–Jones interactions with the parameters determined by the geometric mean of the solvent and solute parameters for both ϵ and σ.

The Simulations. The sequence of simulations with methane through octane as the solute started with an equilibrated configuration of 216 water molecules at ambient conditions, 300 K and 997 kg/m^3. The equations of motion were integrated by using an iterated form of the Beeman algorithm (22) with a time step of 1 fs. The orientational degrees of freedom were described with quaternions (23, 24). The temperature was maintained by using separate Nosé–Hoover thermostats for the translational and for the orientational degrees of freedom (25). Alkanes were introduced sequentially by first replacing one solvent molecule by a methane. This step was followed by an equilibration run of 10 ps to allow the system to relax to a stable configuration with the volume held fixed. Then a production run was initiated.

The next member of the sequence, ethane, was generated by replacing a solvent molecule that is next to the methane by an alkane unit at the proper distance from the methane. Again a 10 ps stabilization run preceeded the production run.

The third member of the sequence, propane, was generated by replacing a near neighbor solvent molecule in an ethane–solvent configuration with an alkane unit at the proper distance and orientation from the ethane. The stabilization run was now 20 ps or longer as the disruption of system caused by this replacement was larger than the disruption in the first two cases.

This replacement, stabilization, and production set of operations was repeated sequentially until one octane and 208 solvent molecules were present. The replacements were made on "equilibrated" systems. This method of introducing alkanes into the water molecules was used because the probability of finding a cavity of the proper size is vanishingly small, even for methane (9).

Each simulation was run for 100 ps, with a sample of the solute environment taken at 0.1-ps intervals, so averages are based on 1,000 samples. The sample consists of the coordinates of the solute and the coordinates of the solvent molecules that are near neighbors of the solute. For convenience, all coordinates are relative to the center of mass of the solute. A near-neighbor solvent molecule is one with the center of mass of the solvent molecule within a specified distance, d_n, of one of the carbon sites of the solute. The distance d_n is taken to be the position of the minimum in the methane–solvent pair function and is 0.5 nm for water. The solvent molecules identified in this way form a solvation shell around the solute.

Various properties of the solvation shell have been determined, including the number of solvent molecules in the shell and the radii of gyration of the solvation shell. Also, the conformation of the solute (butane through octane) has been determined.

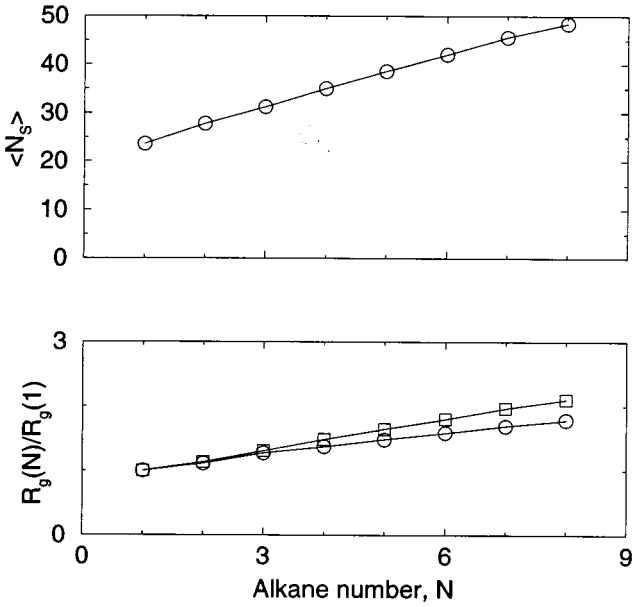

FIG. 1. The average number of molecules, $\langle N_S \rangle$ in the solvation shell is shown for alkane numbers from 1 to 8. The ratio of the major radius of gyration for the alkanes relative to methane (squares) and the corresponding ratio for the minor radius of gyration (circles) are also shown. The lines are to guide the eye.

The average number of solute molecules, $\langle N_S \rangle$, and the major radius of gyration, R_3, and the minor radius of gyration, R_1, of the solvation shells are shown in Fig. 1 as a function of the alkane number. R_3 and R_1 are the mean values of the square roots of the largest and smallest principal components of the inertia tensor averaged over each realization of the solvation shell. The values for individual samples are rather widely distributed with spread of about 10% about the mean value. The conformation of the alkane fluctuates considerably during the 100-ps run, but the solutes do not collapse in water. Fig. 2 shows a snapshot of heptane and the water molecules forming the solvation shell in a typical conformation.

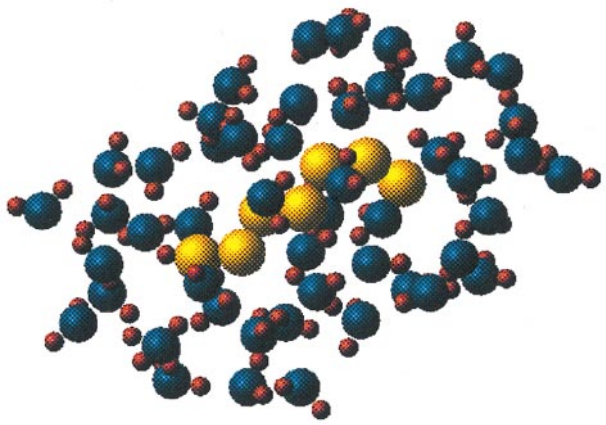

FIG. 2. A snapshot of the instantaneous configuration of heptane in its water hydration shell. The heptane molecule is predominantly in the extended conformation with most of the dihedral angles in the *trans* conformation. The fluctuations at the end of the chain drives the last bond to be in the *gauche* conformation for this configuration. Such transitions appear to occur frequently, although these simulations are too short to generate adequate statistics on these transitions. The water shell contains fragments of rings of hydrogen-bonded molecules, suggesting that short-lived, clathrate-like structures exist. However, in most cases the solute exists in cavities without the terahedral network being compromised.

The number of molecules and the radii of gyration of the shell increases with the number of carbon atoms in the alkane. There is little correlation between the orientation of the principal axes of the solvation shell with the end-to-end orientation of the alkane. We also determined the mean lifetime of a water molecule in the hydration shell. The mean lifetime was determined by using a linear time-weighted distribution of first-passage times. Thus, a larger weight is given to those water molecules whose residence times in the hydration shell are long. We find the mean lifetimes to be on the order of 40 ps. The fluctuations in the lifetimes are found to be on the order of 30 ps, implying that there is a substantial range in the exchange rate of water between the hydration shell and the bulk.

RESULTS

Shape Fluctuations. A simple measure of the anisotropy of the solvation shell can be obtained by calculating the radius of gyration from the inertia tensor of the shell. For small-sized alkanes, the hydration shell is expected to be spherical if the time-averaged inertia tensor is used to determine the principal components. However, if the ensemble averaging is done after the principal components are determined, the intrinsic anisotropy of the hydration shell can be inferred. We have followed the second approach. This measure shows that as the length of the alkane chain increases the solvation shell becomes more anisotropic. In particular for methane and ethane one obtains roughly a spherical solvation shell. If we define an anisotropy parameter $\lambda = R_3/R_1$ where R_3 and R_1 are the major and minor radii of gyration, then we find that λ varies from about 1.10 to 1.30 as the alkane size increases from methane to octane. Although the solvation shells for methane and ethane provide nearly spherical cavities on average, the solvation shells for the higher alkanes are decidedly nonspherical. This result implies that two length scales are required to describe the hydration of the larger hydrocarbons. The volume occupied by the hydration shell also increases monotonically as the size of the hydrocarbon increases. This would suggest that there may be some alteration of the water structure around the larger hydrocarbons.

Plasticity of Hydrogen Bond Network. The rearrangement in water structure as a result of accommodating the solute of given size was examined by probing the structure of the hydrogen bond network. The possible alterations in the hydrogen bond network were examined by considering only those water molecules that are in the hydration shell. Recent reports on hydration of n-dodecane (18) in water suggest that to a large extent the solubilities of relative large nonspherical solutes can, in principle, be understood in terms of cavity statistics. However, the structural changes in the hydrogen bond network close to the solute were not probed (18). To explicitly shed light on the nature of hydrogen-bonded network of water in the immediate vicinity of the solute, we have calculated the distribution of angles θ between three near-neighbor oxygen atoms. The oxygen atoms are required to be within 0.5 nm of at least one of the carbon atoms, i.e., they belong to the hydration shell. Also, two of the oxygens are near neighbors of the oxygen at the vertex of the angle. In Fig. 3 we plot the probability distribution as a function of $\cos\theta$ for octane. For comparison, the distribution of $\cos\theta$ in pure water is also presented. The distribution function in both cases has a peak around the terahedral value ($\cos\theta \approx -1/3$). Even the widths of the distribution functions, which give the fluctuations in $\cos\theta$, are quite similar. This suggests that there is not a significant distortion of the hydrogen-bonded network of water around the solute. The plasticity of the hydrogen-bonded network appears to be crucial in determining the hydrophobic interaction.

The relatively small perturbation of the hydrogen-bond network after accommodating the hydrocarbon solvents can be further inferred by comparing $g_{OH}(r_{OH})$ for the bulk liquid with $g_{OH}(r_{OH})$ obtained for molecules in the hydration-shell only. In Fig. 4, these radial distribution functions are plotted as a function of r_{OH} for octane. The height of the first peak in the hydration shell pair function $g_{OH}(r_{OH})$ is scaled to coincide with that feature of the bulk $g_{OH}(r_{OH})$. Fig. 4 shows that the positions and widths of the two peaks of these two functions are nearly the same. This result is consistent with the physical picture that the hydrogen-bond network is preserved even when accommodating large hydrocarbon solutes.

Although the disturbance in the hydrogen-bond network near the solute is minimal, there is some evidence for slight distortion of the water structure within one layer of the solute. This is most clearly seen in the distribution of C–H and C–O

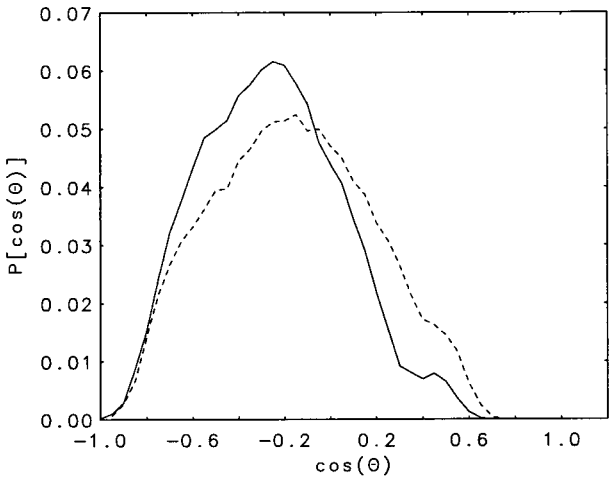

FIG. 3. Distribution of $\cos\theta$ for octane hydration shell with θ being the angle between three oxygen atoms. The solid line corresponds to the distribution function calculated by requiring the oxygen atoms to be within the hydration shell. The dashed line is the distribution function for pure water. Interestingly, in the presence of the octane both the peak and the width of this distribution are nearly the same as in pure water, suggesting very little alteration of the local water structure.

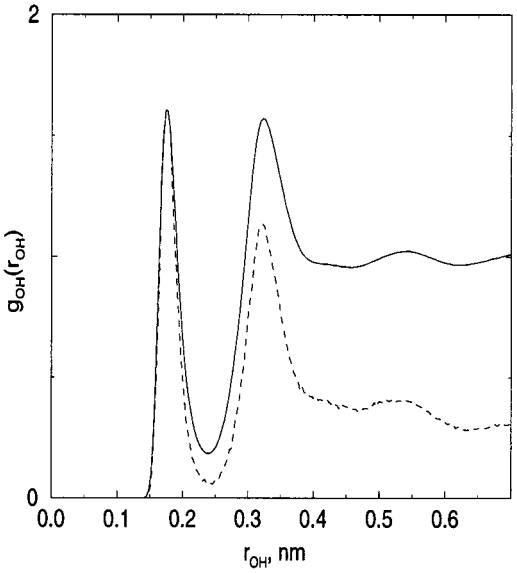

FIG. 4. Plots of the oxygen–hydrogen radial distribution function $g_{OH}(r_{OH})$ are displayed as of function of the oxygen–hydrogen distance r_{OH}. The solid line is for bulk water. The dashed line is obtained by considering only those water molecules that are within the hydration shell of octane. The amplitude of the dashed curve has been scaled so that the heights of the first maxima of the two curves coincide.

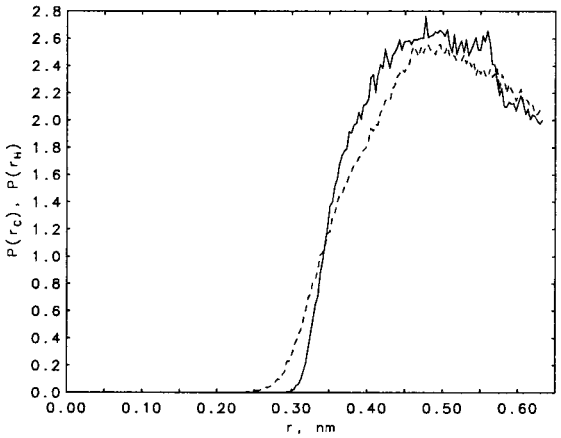

FIG. 5. The distribution of C–O distances, $P(r_C)$ (solid line), and the distribution of C–H distances, $P(r_H)$ (dashed line) are shown for an octane molecule in water.

distances, $P(r_C)$ and $P(r_H)$, of water molecules within the hydration shell. These distributions are displayed in Fig. 5, where we note that a small fraction of the water molecules has their hydrogen atoms closer to the carbon atoms than their oxygen atoms. These hydrogen atoms are not available to participate in the hydrogen bonds, which results in minor changes in the water structure close to the solute. The distributions of hydrogen bond lengths and deviations from linearity for bonds between solvation-shell molecules (not shown) are essentially the same as those in the bulk liquid. These distribution functions show that the hydrogen-bond network is sufficiently flexible so that it can accommodate relatively large hydrophobic species. It is this plasticity that gives water it's unique hydration properties.

Distribution of COC Angles. The geometry of the solute–solvent clathrate structure in the hydration shell can be further characterized by the distribution of the angles χ_{ij} between carbon atoms i and j and the oxygen atoms in the solvent shell. The results for octane are shown in Fig. 6. For almost all the (ij) pairs, the distribution function has a peak at $\cos\chi_{ij} \approx 0.6$ or $\chi_{ij} \approx 53^\circ$. Matubayasi has suggested that spherical hydrophobic solutes are largely found in the cavities corresponding to the "mismatching" regions of the water molecules (26). These "mismatching" regions are defined to be ones for which a triplet of water molecules inhibits the tetrahedral nature of the bulk water. These regions were identified by examining the distribution of angles between triplets of water molecules in which the central water molecule is hydrogen bonded to the other two. The values of $\chi_{ij} \approx 53^\circ$ are predominantly in the mismatched regions. Thus, even for connected, flexible hydrocarbons the monomer units appear to be in the cavity regions in which the distortion of the hydrogen-bond network is minimized.

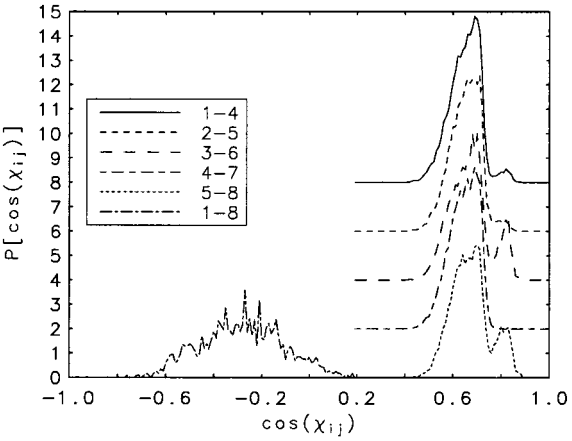

FIG. 6. Probability distribution of $\cos(\chi_{ij})$ for octane where χ_{ij} is the angle between carbon atoms i and j (as indicated in the legend) and an oxygen atom that is in the hydration shell. Note that the curves for 1–4 through 5–8 are offset so that the structure around $\chi_{ij} \approx 0.8$ is evident. For almost all of the i–j pairs, the peak is in a region in which the tetrahedral nature of pure water is maximally compromised. Thus large solutes are in "mismatching" regions as defined by Matubayasi (26). This also is evidence for the plasticity of the hydrogen-bond network.

Probing Direct Solvation of Nonbonded Carbon Atoms. One of the hallmarks of the hydrophobic interaction between methane molecules is the presence of the solvent-separated minimum in the potential of mean force (3, 7). Although such solvent-separated minima are not expected to be relevant in short-chain hydrocarbons, one might argue that for sufficiently large chains the interactions between nonbonded carbon ($|i-j| \geq 3$, where i and j refer to positions of the carbon atoms along the alkane chain) atoms along the chain may be mediated by water. It is such water-mediated interactions that should cause collapse of sufficiently long hydrocarbon chains into globular shapes. We have used various probes to explore the possibility that water causes a large change in the shape of alkanes, with emphasis on octane.

Collapsed conformations can be characterized by a reduction in the size of the hydrocarbon relative to the conformation in which all bonds are in the trans state. We find that the size, as measured by the mean end-to-end distance, $\langle r_{18}^2\rangle^{\frac{1}{2}}$, for octane is reduced by about 10%, i.e., $\langle r_{18}^2\rangle^{\frac{1}{2}}/r_{18}^t \approx 0.9$, where r_{18}^t is the end-to-end distance with all bonds in the trans conformation. By contrast, the size of the octane in which all bonds are in the gauche conformation is about 20% less than r_{18}^t. Since in the collapsed state all bonds are expected to be in the gauche conformation, it follows that the size of the hydrated octane molecule is similar to that in the gas phase.

To gain additional insight into the nature of conformations of octane in water, we have computed the fraction of the time that each torsion angle is in the gauche conformation ($\phi > 60^\circ$). During the course of three independent trajectories of 100 ps duration each, we find no examples of a fully collapsed conformation. This result also suggests that the average size of hydrated octane is similar to that in the gas phase.

To explore the possibility of water-mediated interactions between nonbonded carbon atoms, we have calculated the occupation probabilities of water molecules within a specified distance between two chosen carbon atoms. Specifically, we constructed

$$P(r_{ij}) = \sum_l \Theta[r_c - |r_i - r_l^o|]\Theta[r_c - |r_j - r_l^o|], \qquad [6]$$

where r_l^o is the position of the lth oxygen atom in the hydration shell, r_i and r_j are the positions of the ith and jth carbon atoms, respectively, r_{ij} is the distance between the carbon atoms i and j, r_c is a cutoff distance, and $\Theta[x]$ is the Heavyside function. Thus, molecule l contributes to $P(r_{ij})$ if water molecule l is within a cutoff distance of both the carbon atoms. This correlation function gives an indication of water-mediated interactions between the carbon atoms that are not covalently bonded to each other.

In Fig. 7, we plot $P(r_{ij})$ for various choices of i and j for octane in water. In the upper plot, the lines are the distribution functions given by Eq. **6** for i–j sites 1–4, 2–5, 3–6, 4–7, and 5–8 from the lower to the upper curve. The distributions have been offset by one unit. The lower plot is for the end sites, 1–8. In some of the curves, there is a very small feature at $r_{ij} \approx 0.32$ nm. In most of the cases, it is seen that such distorted conformations, which are required if water-mediated contacts are relevant, occur with relatively low probability. The only exception to this is the pair of carbon atoms

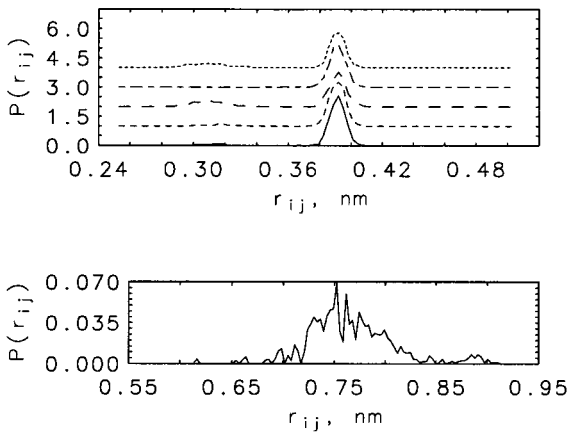

FIG. 7. Distribution function $P(r_{ij})$ (see Eq. **6**) measuring the probability that carbon atoms i and j interact by a solvent mediated mechanism. This figure is for octane. With the possible exception of pair $i = 5$ and $j = 8$, there appears to be no water-mediated contact between nonbonded carbon atoms. Such interactions are probably necessary to induce change in the conformation between an extended random coil to a compact globular phase. This result suggests that this can occur only for linear hydrocarbons of much larger length.

5 and 8. We believe that this is basically due to enhanced fluctuations of the distance between the ends of the molecule and is not indicative of the actual solvation-mediated interactions between these carbon atoms. We find similar results for smaller hydrocarbons. This lack of water-induced interactions between nonbonded carbon atoms is consistent with the idea that the solute is accommodated with very little disturbance of the surrounding structure of water molecules. For sufficiently large alkane chains, we expect a water-induced collapse of the chain into compact globules. The chain length at which the transition from an extended object to a compact globule occurs is not known. All of the probes of chain conformations indicate that water-mediated interactions, which can drive collapse of the chain, can become relevant only when the length of the chain is greater than the lengths considered here.

We wish to add a caveat to this conclusion about the lack of water-mediated interactions between nonbonded carbon atoms. This conclusion is based on trajectories of 100-ps duration. It is useful to compare this time to the time needed for two nonbonded atoms to diffuse within a distance such that interactions mediated by a single water molecule become possible. The diffusion time scale for sites separated by three atoms is in the range of 1.5 ps to 15 ps if we assume that the mutual diffusion coefficient is on the order of 10^{-10} m^2/s to 10^{-9} m^2/s. This time is less than the duration of our simulations. Nevertheless, we cannot rule out the possibility that on a longer time scale such water-mediated interactions occur with significant probability.

CONCLUSIONS

In this article, we have undertaken a study of hydration of small hydrocarbons by using molecular dynamics simulations. For all the hydrocarbon molecules (methane to octane) introduced into the solvation shell, the solute molecules undergo fluctuations in their conformations without significantly perturbing the local water structure. We find that there are no major structural changes in water compared to the bulk or pure water. The plasticity of the hydrogen-bond network suggests that hydration of even large solutes can be understood in terms of cavity statistics; this is an inherent assumption of scaled particle theory and theories based on integral equations (7). From the present and previous studies (8, 9, 18), it appears that the hydrophobic interaction arises primarily from *the strong tendency to preserve the hydrogen bond network.* As a consequence, the fluctuations in cavity sizes in water are inherently smaller than in other liquids.

It is interesting that the structure of water is hardly perturbed by the presence of the solutes. Even for the largest hydrocarbon considered here, namely octane, very minor changes in the various correlation functions describing the water structure are observed. This is consistent with the results of Wallqvist and Berne (27), who also suggested that the structure of water is not significantly altered close to large hydrophobic ellipsoidal plates. The only penalty is the decrease in the entropy due to the excluded volume of the solutes.

We are grateful to L. R. Pratt and P. J. Rossky for useful comments. Discussions with L. R. Pratt were critical in our understanding of different viewpoints of the hydrophobic effect found in the literature. The critical reading of this paper by Anneke Levelt Sengers is greatly appreciated.

1. Dill, K. A. (1990) *Biochemistry* **29,** 7133–7155.
2. Tanford, C. H. (1980) *The Hydrophobic Effect* (Wiley, New York).
3. Pangli, C., Rao, M. & Berne, B. J. (1979) *J. Chem. Phys.* **71,** 2975–2981.
4. Pangli, C., Rao, M. & Berne, B. J. (1979) *J. Chem. Phys.* **71,** 2982–2990.
5. Zichi, D. A. & Rossky, P. J. (1985) *J. Chem. Phys.* **83,** 797–808.
6. Zichi, D. A. & Rossky, P. J. (1986) *J. Chem. Phys.* **84,** 2814–2822.
7. Pratt, L. R. & Chandler, D. (1977) *J. Chem. Phys.* **67,** 3683–3704.
8. Pratt, L. R. & Pohorille, A. (1992) *Proc. Natl. Acad. Sci. USA* **89,** 2995–2999.
9. Hummer, G., Garde, S., García, A. E., Pohorille, A. & Pratt, L. R. (1996) *Proc. Natl. Acad. Sci. USA* **93,** 8951–8955.
10. Lazaridis, T. & Paulaitis, M. E. (1994) *J. Phys. Chem.* **98,** 635–642.
11. Pollack, G. L. (1991) *Science* **251,** 1323–1330.
12. Pierotti, R. A. (1978) *Chem. Rev.* **76,** 717–726.
13. Stillinger, F. H. (1973) *J. Solution Chem.* **2,** 141–158.
14. Madan, B. & Lee, B. (1994) *Biophys. Chem.* **51,** 279–289.
15. Lee, C. Y., McCammon, J. A. & Rossky, P. J. (1984) *J. Chem. Phys.* **80,** 4448–4455.
16. Wallqvist, A. & Berne, B. J. (1988) *Chem. Phys. Lett.* **145,** 26–32.
17. Wallqvist, A. (1991) *Chem. Phys. Lett.* **165,** 437–442.
18. Wallqvist, A. & Covell, D. G. (1996) *Biophys. J.* **71,** 600–608.
19. Berendsen, H. J. C., Grigera, J. R. & Straatsma, T. P. (1987) *J. Phys. Chem.* **91,** 6269–6271.
20. Smit, B., Karaborni, S. & Siepmann, J. I. (1995) *J. Chem. Phys.* **102,** 2126–2140.
21. Clarke, J. H. R. & Brown, D. (1986) *Mol. Phys.* **58,** 815–825.
22. Schofield, P. (1976) *Comput. Phys. Commun.* **5,** 17–23.
23. Sonnenschein, R. (1985) *J. Comput. Phys.* **59,** 347–350.
24. Rapaport, D. C. (1985) *J. Comput. Phys.* **60,** 306–314.
25. Martyna, G. J., Klein, M. L. & Tuckerman, M. (1992) *J. Chem. Phys.* **97,** 2635–2643.
26. Matubayasi, N. (1994) *J. Am. Chem. Soc.* **116,** 1450–1456.
27. Wallqvist, A. & Berne, B. J. (1995) *J. Phys. Chem.* **99,** 2893–2899.